9

Hydrogeology of the Galápagos Archipelago: An Integrated and Comparative Approach Between Islands

Sophie Violette[1,4], Noémi d'Ozouville[1,2], Alexandre Pryet[1], Benoît Deffontaines[3], Jérôme Fortin[4], and Mathilde Adelinet[5]

ABSTRACT

In this paper, we present an original synthesis of recent hydrogeological studies of the Galápagos Islands. We compare and contrast hydrological data from two Galápagos Islands, San Cristóbal and Santa Cruz, for which no baseline data existed prior to the start of the Galápagos Islands Integrated Water Studies project (GIIWS) in 2003. Two complementary datasets are considered in this work, collected using direct methodologies (*in situ* measurements at watershed-scale experimental sites) and indirect methodologies (satellite imagery interpretation, helicopter-borne geophysics acquisition at regional scale). Using these datasets, we:

1. Present a synthesis of the hydrogeology of San Cristóbal and Santa Cruz;
2. Explain differences in their hydrodynamic functioning; and
3. Explore the implications of these results for water resource management on the Galápagos inhabited islands.

We propose that a number of key factors, including geomorphology, near-surface lithology, and age, control the primary hydrological similarities and differences between San Cristóbal and Santa Cruz. Finally, we propose that the distribution and occurrence of groundwater resources on San Cristóbal and Santa Cruz define an evolutionary link between the two classical conceptual hydrogeological models (the Hawaiian model and the Canary Islands model) proposed in the literature for basaltic islands. Indeed, Santa Cruz is similar to the Hawaiian model (valid for young islands under 1 Ma) and San Cristóbal is an advanced stage of the Hawaiian model that is evolving toward the Canary Islands model (valid for old islands over 5 Ma).

9.1. INTRODUCTION

The hydrogeology of basaltic islands remains poorly understood, partly due to their intrinsic complexity and the difficulty of collecting sufficient data to adequately characterize their hydrodynamic functioning. Indeed, the internal structure of basaltic islands reflects a succession of constructional and dismantling phases, interrupted by quiet periods when weathering processes are dominant. At depth, hydrothermal activity in volcanic edifices can induce mineral transformations in surrounding areas [*Keller et al.*, 1979], accompanied on the surface by hot springs and fumaroles. Furthermore, in tropical and equatorial climates, these islands are densely vegetated, making their steep inland slopes difficult to investigate.

As a result of the growth of the tourism industry and the need for water resources in the past few decades, economic development on volcanic islands has accelerated, particularly along the coasts. After centuries of isolation, the Galápagos Archipelago is no longer an exception to this scenario. Five of the islands are inhabited (San Cristóbal,

[1] *UPMC-Sorbonne Universités and CNRS, UMR. 7619-Sisyphe*
[2] *Charles Darwin Foundation*
[3] *Université de Marne-la-Vallée, Laboratoire GTMC*
[4] *Ecole Normale Supérieure and CNRS, UMR.8538-Laboratoire de Géologie*
[5] *IFP Énergies nouvelles*

The Galápagos: A Natural Laboratory for the Earth Sciences, Geophysical Monograph 204. First Edition.
Edited by Karen S. Harpp, Eric Mittelstaedt, Noémi d'Ozouville, and David W. Graham.
© 2014 American Geophysical Union. Published 2014 by John Wiley & Sons, Inc.

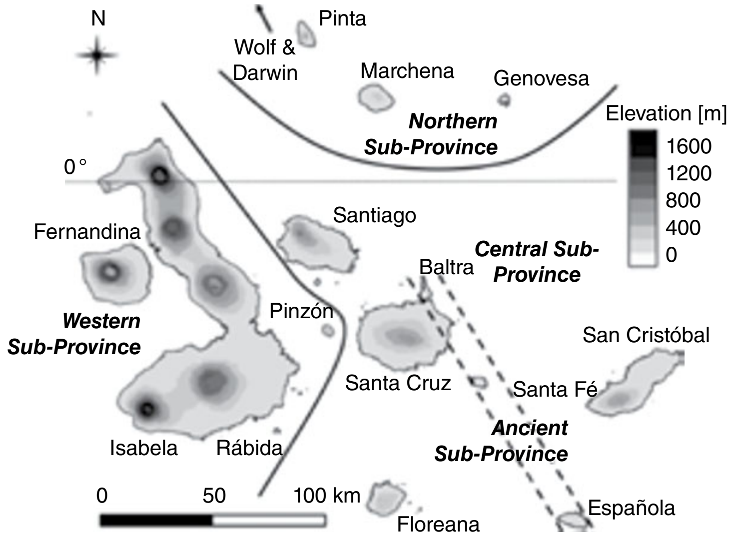

Figure 9.1 Galápagos Archipelago location and geological provinces defined by McBirney and Williams [1969], DEM SRTM 90 m [http://seamless.usgs.gov], coastal line geo-referenced by *CDF et al.* [2004].

Santa Cruz, Floreana, Isabela, and Baltra) and face critical issues regarding water shortages and quality (Figure 9.1). Thus, learning more about Galápagos hydrogeology is crucial not only to improve the scientific understanding of basaltic island hydrogeology, but also to develop locally sustainable water resource management practices.

Two conceptual hydrogeologic models are commonly invoked to explain the occurrence of groundwater in basaltic insular environments:

1. The Hawaiian model, developed by *Peterson* [1972], improved by *MacDonald et al.* [1983] and then applied successfully to other islands, including French Polynesia [*Pouchan et al.*, 1988; *Hildenbrand et al.,* 2005], La Réunion [*Stieljes et al.*, 1988], the young Piton de la Fournaise–La Réunion [*Violette et al.*, 1997], Madère [*Prada et al.*, 2005], and Cape Verde Island [*Heilweil et al.*, 2009]; and
2. The Canary Islands model, developed by *Custodio et al.* [1983, 1988] and applied successfully to the old Piton des Neiges–La Réunion [*Join et al.*, 1997], the young Piton de la Fournaise–La Réunion [*Join et al.*, 2005], Jeju–Korea [*Won et al.*, 2005], Easter Island–Chile [*Herrera et Custodio*, 2007], and Kauai–Hawai'i Archipelago [*Izuka and Gingerich*, 2003].

In the Hawaiian model, the basal aquifer, in equilibrium with the ocean, presents a weak hydraulic gradient even far inland due to the basalt's high hydraulic conductivity. Inland and above the basal aquifer, the presence of dikes or low permeability layers favors dike-compartmented or perched aquifers. In the Canary Islands model, the hydraulic gradient of the basal aquifer follows surface topography and remains at shallow depth due to decreasing hydraulic conductivity with depth. Both models have important implications for groundwater exploitation and management. In the Hawaiian model, the basal aquifer is often brackish along the coast, its exploitation inland is costly due to its depth, and the presence of perched aquifers inland makes them challenging to locate. In the Canary Islands model, the basal aquifer can be reached by boreholes or drainage galleries at shallow depths anywhere on the island.

Whereas many factors influence the hydrogeology of a basaltic island, including age, climate, near-surface lithology, weathering, tectonic-volcanic constructional and destructive processes, and erosion, little is known about the relative importance of each parameter; the Galápagos Archipelago offers an opportunity to define which of these factors most affects the hydrogeological potential of volcanic islands. (Throughout this paper, the term "hydrogeological potential" is defined as the occurrence of groundwater and/or freshwater aquifers). Since 2003, Santa Cruz (SZ) and the southwestern part of San Cristóbal (SC) islands have been the focus of the GIIWS project, lead by UPMC-Sorbonne Universités. By all appearances, these two islands are built from similar basalt rock and are exposed to comparable equatorial climate conditions. There are, however, some relatively minor but important differences between the islands. The ages of the more recently erupted lavas are older on San Cristóbal (2.35 Ma) [*Geist et al.*, 1986] than on Santa Cruz (1.3/0.59–0.05 Ma) [*White et al.*, 1993]. The nature and thickness of the weathered cover also differ, with 1 m on Santa Cruz compared to 10 m on San Cristóbal [*Geist et al.*, 1986]. More importantly, the two islands present very different hydrological characteristics. Perennial springs feed a drainage network on San Cristóbal, which also has a permanent freshwater lake in a crater, while permanent surface water is absent on Santa Cruz and groundwater resources are restricted to a brackish basal aquifer along the coast and a small spring issuing from a volcanic cone inland (Table 9.1).

Table 9.1 Primary climatic, physiographic, geomorphologic, hydrological, and hydrogeological features of Santa Cruz and San Cristóbal Islands.

Climate
Garua: cool & dry, Jun.-Dec.
Invierno: hot & rainy, Jan.-Jul.
Inter-annual rainfall windward side
Alt. 0 m–500 mm
Alt. 180 m–1630 mm
Alt. 400 m–2400 mm
Alt. 650 m–3070 mm
El Niño extreme event
Rainfall × 4

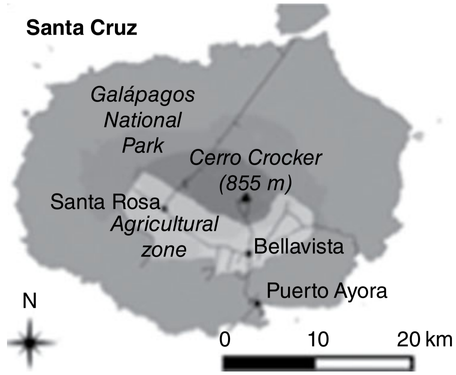

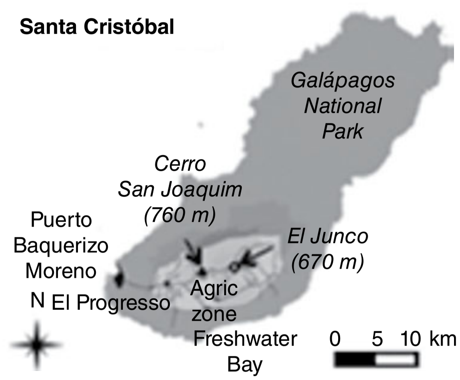

	Santa Cruz	Santa Cristóbal
Geomorphology		
Age	1.3/0.59-0.05 Ma	2.35 Ma
Surface	986 km^2	558 km^2 (Southern part ~275 km^2)
Form	sub-circular	elongated
Peak	855 m	760 m
Slopes	< 2* coast (apron) > 5* highlands	no apron > 5* coast & highlands
Park land territory	88%	84%
Agriculture & urban zones	12%	16%
Hydrology		
Ravine Pond	no perennial surface flow brackish ponds (coast); no perennial freshwater ponds and bogs (highlands)	perennial surface flow brackish ponds (coast); perennial and non perennial freshwater ponds (highlands); perennial El Junco Lake
Hydrogeology		
Basal aquifer	access by "*grietas*" and "*pozos*"; weak hydraulic gradient (coast), $i = 5.10^{-5}$ identified up to 9 km inland; contaminated by seawater intrusion and urban waste water	revealed by *Skytem* survey; weak hydraulic gradient identified up to 9 km inland brackish
Perched aquifer Spring	revealed by *Skytem* survey one cone spring (Santa-Rosa)	revealed by *Skytem* survey numerous perennial freshwater springs, low flow rates

In this paper, we present a comprehensive synthesis of Galápagos Islands hydrogeology. As part of the GIIWS project, we identify the key factors that explain the primary hydrological similarities and differences between the two islands through analysis of recent hydrological studies, *in situ* measurements of watershed-scale experimental sites, satellite imagery interpretation, and heli-borne geophysics acquisition. These data also define a critical baseline set of observations that did not exist prior to the initiation of the GIIWS project, which is essential for future studies and development of water management practices.

9.2. CONSTRAINTS OF BASALTIC ISLANDS AND ADVOCATED METHODOLOGY

In addition to their intrinsic complexity, basaltic islands in equatorial and tropical climates are difficult to investigate due to their dense vegetation cover, steep slopes, and hard basement rock coupled with wide cavities such as lava tunnels that are often encountered even at depth during drilling. Consequently, over the past few decades, a variety of indirect methods have been developed and tested to study basaltic islands to complement classical ground-based investigations. These methods include remote sensing [*Peireira et al.*, 2007], geophysical exploration [*Descloitres et al.*, 1997], isotopic [*Scholl et al.*, 1998], noble gas geochemistry [*Marty et al.*, 1993], hydrogeological modeling [*Custodio et al.*, 1988], and coupled flow and thermal modeling [*Violette et al.*, 1997].

In the Galápagos Archipelago, 97% of the terrestrial area is protected national park land. Prior to the initiation of the GIIWS project in 2003, there was no ground-based hydrologic data collection, except for inventory mapping of Galápagos natural resources (INGALA et al., 1989). Recent studies have employed novel ground-based and indirect methodologies in the Galápagos to construct a hydrogeological conceptual model [*d'Ozouville*, 2007; *Pryet*, 2011] (Figure 9.2), demonstrating the value of integrating tools from a variety of disciplines (including geology, remote sensing, geophysics, climatology, hydrology, and hydrochemistry).

Despite these efforts, high-resolution topographic data sets are still lacking in the Galápagos Islands. The most comprehensive existing dataset is the Shuttle Radar Topographic Mission (SRTM) 90 m resolution data, available since 2004. These data were combined with ENVISAT radar acquisitions over the Galápagos Islands to assemble a 20 m resolution digital elevation model (DEM) of Santa Cruz [*d'Ozouville et al.,* 2008a]. Horizontal and vertical accuracy (15 m and 10 m, respectively) was validated using ground-based control points. Watershed limits and surface drainage networks extracted from this DEM were verified against ground-based field observations and river networks visually extracted from aerial photographs and high-resolution (1 m) satellite imagery available on Google Earth [2004].

Following a large-scale, ground-based geophysical investigation that had only limited success owing to lack

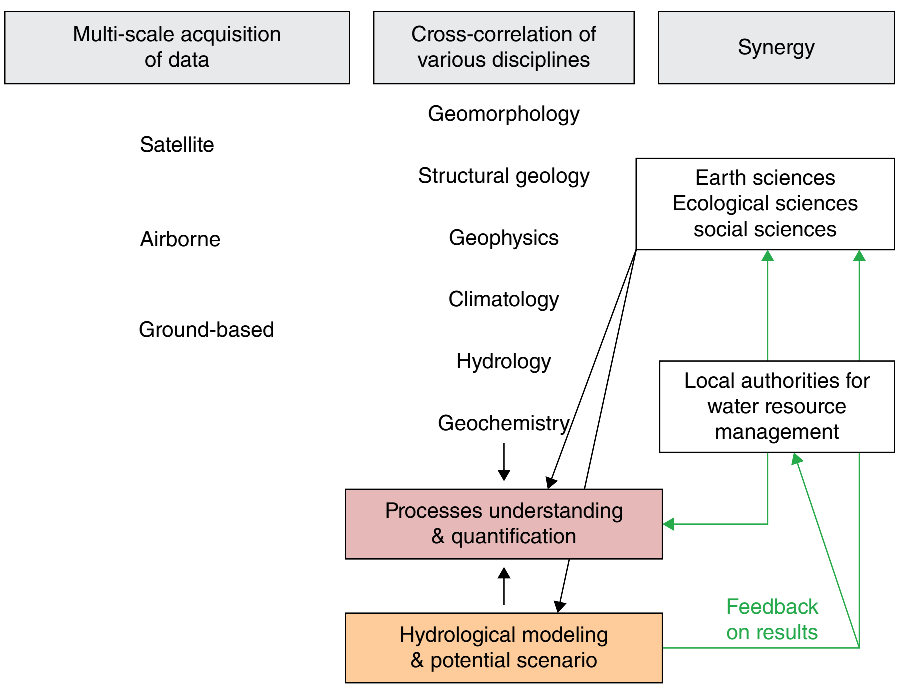

Figure 9.2 Integrated approach recommended for hydrogeological study of volcanic islands.

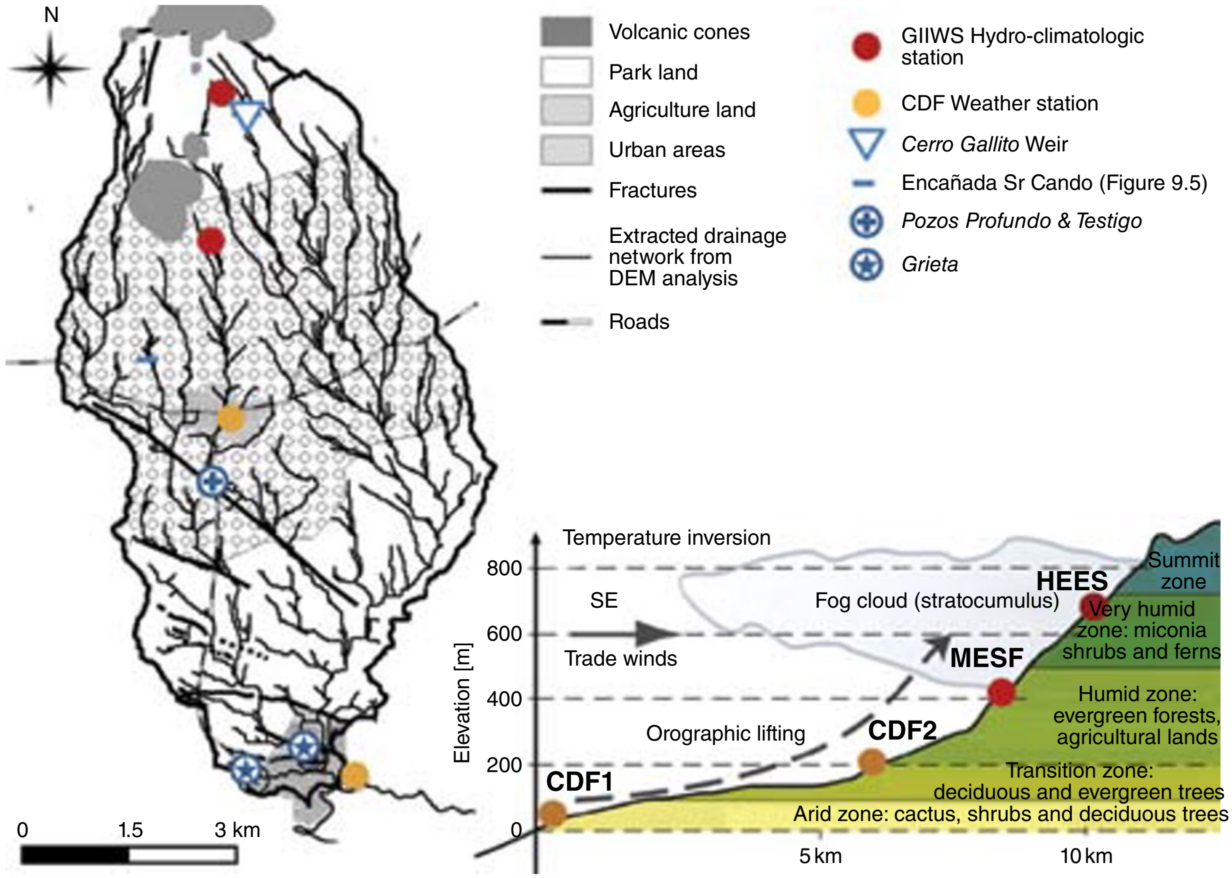

Figure 9.3 Hydro-climatologic network at watershed scale (Pelican Bay watershed on Santa Cruz Island) and vegetation stages along the orographic gradient by *Hamann* [1979] with Charles Darwin Foundation (CDF) weather station and Galápagos Islands: Integrated Water Study (GIIWS) hydro-climatologic station locations.

of access to many parts of the islands, a helicopter-borne transient electromagnetics (SkyTEM) mission was carried out over Santa Cruz and San Cristóbal Islands in May 2006, testing this innovative instrument for the first time on volcanic islands [*d'Ozouville et al.*, 2008b; *Auken et al.*, 2009; *Pryet et al.*, 2012b]. A new technique for three-dimensional visualization of the large, high-resolution resistivity dataset was developed by *Pryet et al.* [2011]. This method allows resistivity ranges to be extracted from the complete dataset, revealing features of the internal structure of the volcanic massifs, including depth to the saltwater interface. The resulting 3D-block diagrams of resistivity can be visualized from different angles and overlain with structural geology information, remote sensing data, and field observations [*Pryet et al.*, 2012b].

The hydrogeological potential (i.e., the presence of the aquifer) of the low resistivity layers (30–100 ohm.m) measured on San Cristóbal was confirmed by a ground-based reconnaissance study and an inventory of perennial springs, the outlet of perched aquifers [*Adelinet*, 2005]. In the absence of borehole validation on Santa Cruz, this identified relationship (between resistivity ranges of a saturated basalt layer and spring occurrence, outlet of perched aquifers) on San Cristóbal was used to determine the hydrogeological potential of the buried low resistivity layer on Santa Cruz [*d'Ozouville et al.*, 2008b; *Auken et al.*, 2009]. To document the hydrodynamic boundary conditions (i.e., recharge rate quantification) of perched, buried aquifers on Santa-Cruz, a hydro-climatic network was set up on the recharge area at two locations: at Mid-Elevation in the Secondary Forest (MESF elevation: 400 m), and at High Elevation in Endemic Shrubs (HEES elevation: 650 m) on the watershed of Pelican Bay (Figure 9.3). These two automatic hydro-climatic stations complement the existing long-term manual stations operated by the Charles Darwin Foundation, which are located at lower altitudes (CDF1 Charles Darwin is at 2 m above mean sea level a.m.s.l. and CDF2 Bellavista is at 180 m a.m.s.l.). This network allows us to quantify the water budget along the orographic gradient of the island and to characterize water transfer in soil or saturated bodies. Mechanisms such as cloud water interception during the cool season, when a permanent inversion layer sets in over 400 m and generates occult precipitation known as *garúa*, have been identified and quantified [*Pryet et al.*, 2012a]. Physical and hydrodynamic properties of the soil along windward slope profiles of both islands also provide insights into the weathering process [*Adelinet et al.*, 2008].

Even though the GIIWS is still in progress, we have collected enough data to offer a comprehensive view of the hydrogeology of San Cristóbal and Santa Cruz Islands. Details of previous results from the GIIWS are available in the references listed above. In this paper, we synthesize results from the GIIWS to date, focusing on the following issues:

1. We present a comprehensive perspective on the hydrogeology of San Cristóbal and Santa Cruz islands;
2. We explain the fundamental hydrodynamic differences between them; and
3. We discuss the implications of our results for water resource management on inhabited Galápagos islands.

9.3. MAIN FEATURES OF SAN CRISTÓBAL AND SANTA CRUZ ISLANDS AND THEIR SIGNIFICANCE FOR WATER RESOURCES

9.3.1. Geology and weathering processes

Located on the equator in the eastern Pacific Ocean, about 1,000 km off the coast of Ecuador, the Galápagos Archipelago emerges from a shallow submarine platform, which forms the western part of the east-west trending Carnegie Ridge on the Nazca plate [*Geist et al.*, 1988; *White et al.*, 1993]. Its origin is due to the activity of a hotspot [e.g., *Hey et al.*, 1977] less than 100 km north, but the presence of a segmented mid-ocean ridge (the Galápagos Spreading Center; GSC) cannot be ignored, as it affects the structure and organization of the islands [e.g., *Morgan*, 1978; *Mittelstaedt and Ito*, 2005; *Harpp and Geist*, 2002]. The archipelago is composed of fifteen islands that have been sub-divided into four geological sub-provinces (Figure 9.1) [*McBirney and Williams*, 1969]:

1. Ancient sub-province: Española, Santa Fe, Baltra, NE Santa Cruz, North Seymour;
2. Central sub-province: San Cristóbal, Santa Cruz, Santiago, Floreana;
3. Western sub-province: Isabela, Fernandina, Pinzón, Rábida;
4. Northeastern sub-province: Pinta, Genovesa, Marchena, Wolf, Darwin.

The northeast corner of Santa Cruz Island is covered by the Platform Series lavas, which belong to the Ancient sub-province and are the oldest exposed material on the island (1.3 Ma) [*White et al.*, 1993; *Bow*, 1979]. The surface lavas on the rest of the island belong to the Shield Series, which is assigned to the Central sub-province; these lavas are younger than the Platform Series (0.56–0.05 Ma) [*White et al.*, 1993; *Bow*, 1979]. The southern shield of San Cristóbal first emerged approximately 2.35 ± 0.03 Ma ago, whereas the northeastern half of the island was formed during the Holocene [*Geist et al.*, 1986; *White et al.*, 1993]. Neither Santa Cruz nor the southern part of San Cristóbal has experienced any eruptions in the past 10,000 years, but both may still be considered active [*White et al.*, 1993]. Built from alkaline basalt deposited during effusive events, these smooth shield volcanoes have no summit calderas. The highlands of Santa Cruz are characterized by steep slopes (more than 5°) and bounded on the coast by an asymmetric, north-south, low slope apron (less than 2°). The southern part of San Cristóbal is characterized by steep slopes (more than 5°) and is devoid of a low-lying coastal apron. Unlike Santa Cruz Island, the summit area of San Cristóbal was covered by thick pyroclastic deposits (up to 10 m) at the end of its volcanic activity around 0.6 Ma [*Geist et al.*, 1986].

On its windward side, Santa Cruz is covered by a thin weathered layer (i.e., soil), with thicknesses that vary in a lens shape with elevation (0 m along the coast, less than 1 m at mid-slope, and few centimeters at the summit). On San Cristóbal, the combination of thick pyroclastic deposits, damp weather conditions on the windward side, and longer exposure to weathering processes has favored the development of a thick soil layer. The hydrodynamic properties and mineralogical composition of the soil on both islands evolved along the orographic gradient of the windward side, especially between low and high altitudes, as demonstrated by *Adelinet et al.* [2008]. Above 250 m elevation, chemical alteration under air-water saturation conditions is intense and revealed by the occurrence of gibbsite. The intensity of the chemical weathering process decreases with soil depth where the mineral smectite is preserved. At low altitude (below 250 m elevation), mechanical processes under arid conditions are dominant and the content of clay minerals is low. The hydraulic conductivities were measured on-site, whereas the porosities are estimated in the laboratory on soil-preserved samples and range from 15–25% for the porosity and 10^{-5}–10^{-6} m/s for the hydraulic conductivity (K) in the highlands, but 35–40% and 10^{-3}–10^{-4} m/s, respectively, at low elevation [*Adelinet et al.*, 2008].

9.3.2. Climate and water budget

Because of its equatorial location, the Galápagos Archipelago is characterized by anomalously cool and dry climatic conditions. The observed seasonality is governed by the movement of the Inter-Tropical Convergence Zone (ITCZ) [*Sachs et al.*, 2009], which results in variations of the prevailing south–east (SE) trade winds and

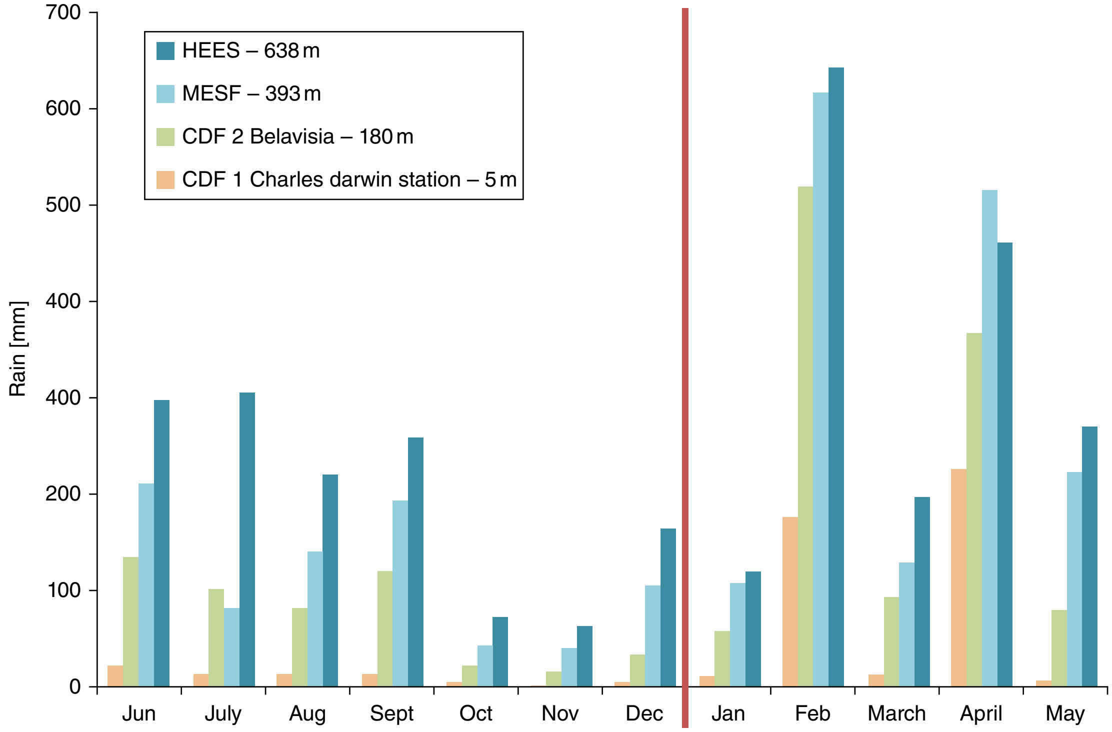

Figure 9.4 Spatial and seasonal variability of monthly rainfall along the orographic gradient, hydrological year 2011–2012, CDF 1 Charles Darwin Station and CDF 2 Bellavista records, MESF and HEES GIIWS station records. Vertical red line separates *garúa* season (left) from *invierno* season (right).

upwelling of the cold Equatorial and Humboldt ocean currents that converge at the archipelago [*Eden and Timmermann*, 2004]. In this region, the El Niño Southern Oscillation (ENSO) induces extreme inter-annual climatic variations. Positive ENSO anomalies result in El Niño events, characterized by increased sea surface temperature, deepening of the thermocline, and a dramatic increase in rainfall on terrestrial areas. During La Niña events, the negative anomalies of ENSO associated with colder-than-average sea surface temperature are characterized by the drought occurrence in the terrestrial areas [*Snell and Rea*, 1999; *Trueman and d'Ozouville*, 2010]. The relief of the volcanic islands creates a stark contrast between the windward side (exposed to the SE trade winds) and the leeward side (protected from the trade winds) of each island. The windward side is more humid than the leeward side; low-lying islands located in the lee of large islands receive rainfall only during exceptionally wet years. The relief also induces an orographic effect on temperature and rainfall [*d'Ozouville*, 2007].

Work on climatology has, until now, been limited in its scope, due to the extreme inter-annual variability observed in the Galápagos, the spatial variability between coast and highlands, and the lack of long-term data records. Two seasons are clearly defined: the cool *garúa* season, from June to December, and the hot *invierno* season, from January to May [*Trueman and d'Ozouville*, 2010]. From a hydrological perspective, the onset of the cool season in June defines the beginning of the hydrological year [*d'Ozouville*, 2007]. During the *garúa* season, the cool air creates an inversion layer and brings a moisture-laden mist above approximately 250 m, whereas below this elevation the lowland areas remain dry. The occurrence and intensity of the fog increases with altitude, and the fog becomes a non-negligible term for the water budget at 650 m, where dense vegetation intercepts it. The fog constitutes 26 ± 16% of the incident rainfall [*Pryet et al.*, 2012a]. During the *invierno* season, rainfall is convective; the amount of precipitation is positively correlated with sea surface temperatures [*Trueman and d'Ozouville*, 2010], the climate is warm with occasional heavy rain showers, and dry spells result in strong evapotranspiration.

The rainfall distribution along the windward side of Santa Cruz Island for the 2011–2012 hydrologic year has been documented (Figure 9.4; Table 9.1) using existing data records from CDF 1 Charles Darwin Research Station and CDF 2 Bellavista (2 m and 180 m elevation, respectively) [www.darwinfoundation.org/datazone/*climate*] and the GIIWS data records at MESF and HEES (400 m and 650 m elevation, respectively). Annual rainfall ranges from 502 mm on the coast to 3068 mm in the highlands. The mean orographic gradient for rainfall is 398 mm per 100 m of elevation from 0–650 m a.m.s.l., but the orographic gradient decreases with elevation (644 mm, 353 mm, and 266 mm per 100 m of elevation between two successive stations from CDF to HEES, taken by pair of stations). These data confirm previous estimates by *d'Ozouville* [2007] and *Pryet* [2011]. The orographic precipitation gradient is well-defined during the cool season, when it is accompanied by wind. In contrast, precipitation during the hot season is convective and can be spatially variable for individual rainfall events.

Compared to the long-term records available at the Charles Darwin Research Station and Bellavista, the 2011–2012 hydrologic year was wetter than average. Available rainfall data on San Cristóbal do not allow calculation of the south-north transect along the windward slope because there are no stations in appropriate locations. Using available data from long-term coastal records, average inter-annual rainfall is 368 mm at Puerto Baquerizo Moreno (6 m a.m.s.l.); applying the orographic gradient observed on the neighboring island of Santa Cruz (SZ), average rainfall is predicted to be 2,961 mm above 650 m of elevation.

Average annual temperatures are 24.0 ± 3.9 °C on Santa Cruz and 24.8 ± 4.3 °C at sea level on San Cristóbal. As a result of seasonality, average temperatures are lower during the *garúa* season (22.6 ± 3.4 °C and 23.5 ± 3.4 °C on Santa Cruz and San Cristóbal, respectively) than in the *invierno* season (26.0 ± 2.0 °C and 26.5 ± 2.7 °C). *d'Ozouville* [2007] observed a temperature gradient of −0.8 °C per 100 m of elevation for Santa Cruz, whereas *Collins and Bush* [2010] report temperature gradients of −0.77 °C per 100 m for the warm season and −0.9 °C per 100 m for the cool season on the south slope of San Cristóbal.

On the basis of these preliminary findings, Potential Evapotranspiration (PET)—the amount of evaporation that would occur if sufficient water were available—was calculated using the Thornthwaite formula for the windward side of Santa Cruz [*d'Ozouville*, 2007]. As expected, annual PET decreases with elevation and its gradient is estimated to be −70 mm per 100 m of elevation, with a mean value of 1,250 mm per year at the coast. Furthermore, PET is lower during the cool *garúa* season, particularly in the highlands, while it increases during the *invierno* season. It is likely that the use of this formula, which only takes into account location and monthly temperature, underestimates the value of PET when compared to calculations that consider daily temperature, solar radiation, and relative humidity, such as the Penman or Turc formulas [*Brochet and Gerbier*, 1968]. The PET is never achieved at low elevation, and effective rainfall (Peff = Rainfall – PET) is reduced during intense rainfall events, which only occur a few times per year. They do occur more frequently during El Niño or extreme rainfall years. For transitional altitudes (150–200 m), PET is occasionally achieved during the *garúa* season and during extreme rainfall events. For higher altitudes (more than 200 m), PET is sporadically achieved during the *garúa* season and during the rainy months of the *invierno* season. Above 400 m, PET is achieved consistently during the *garúa* season and during the wet months of the *invierno* season. Available water for runoff or infiltration, also known as effective rainfall, therefore only occurs above 200 m elevation on a regular basis and its availability increases with elevation.

Vegetation zonation in the Galápagos Islands has always been closely linked to climatic controls and water availability [*Hamann*, 1979] (Figure 9.3). For specific species (i.e., the Scalesia forest), soil properties control the extent of their distribution [*Laruelle*, 1967]. The lowlands, below 150 m, host arid vegetation composed of cactus, shrubs, and deciduous trees. The transition zone, 150–200 m, hosts deciduous and evergreen trees. Anthropogenic evergreen forest and agriculture lands occupy the humid zone, 200–500 m. The very humid zone below the summit hosts the endemic species miconia shrubs and ferns.

9.3.3. Geomorphology and surface hydrology

Surprisingly, as of ten years ago, bathymetric data for the waters surrounding the Galápagos Islands were more accurate than the available topographic data [*INGALA et al.*, 1989]. Now, for Santa Cruz Island, the 20-meter resolution DEM [*d'Ozouville et al.*, 2008a] fills this void and allows extraction of drainage networks, watersheds, and flow characteristics for morpho-structural analysis. Santa Cruz has an area of 986 km^2, of which 88% belongs to the Galápagos National Park (Table 9.1). Maximum elevation is 855 m a.m.s.l., with cinder cone peaks aligned in a NW-SE trend across the island. The island presents an asymmetry between the south and north sides. Two breaks in slope are observed at 200 m and 500 m along the shorter southern side, whereas the ones observed on the northern side are located at 100 m and 600 m. Watersheds with surface areas greater than 5 km^2 (thirty-eight in total) are radially distributed around the island from the crest to the coast and are asymmetric according to their orientation. The extracted drainage network from the DEM [*d'Ozouville et al.*, 2008a] does not correspond to a permanent runoff network, but aligns with known temporary runoff waterways. Fracture analysis of DEM hill shading shows that the drainage network is affected by fractures that act as drains to water flow, but also by massive lava flows, which may form barriers to surface flow.

The runoff occurs sporadically during extreme events (*invierno* season; Figure 9.5) and generates flash floods,

Figure 9.5 View of ravine on Santa Cruz: (A) before, (B) during, and (C) after extreme runoff event Encañada Sr. Cando, February 10–20, 2012 (*photograph N. d'Ozouville*).

which sometimes reach the sea at surface watershed outlets. At those times, stream power is great enough to mobilize blocks and gravels and to destroy vegetation along ravines. This contributes to morphological incision, and over time can play an important role in shaping the landscape. On the highlands during the *garúa* season, a weak surface runoff is maintained along the low permeable bedrock of the ravines above 450 m, which rapidly infiltrates to the pervious fractured basalts when the slope decreases or when the surface flow encounters open vertical fractures. On a small highland watershed, concentration of surface flow was found to be negligible, compared to infiltration processes after accounting for evaporation. For the Cerro Gallito Watershed (Figure 9.3), water balance parameters for the 2005–2006 hydrological year are: 9% runoff, 32% infiltration, and 59% actual evapotranspiration (outflow elevation: 660 m) [*d'Ozouville,* 2007]. These numbers do not take into account the underestimated evapotranspiration, or the contribution to the water budget of cloud water interception by vegetation (see Climate and water budget, above). Below 200 m elevation, effective rainfall is not available on a monthly basis, owing to high potential evapotranspiration demand (see Climate and water budget, above).

The southeastern part of San Cristóbal has an elongated E-W shape and an area of 275 km^2, of which 84% belongs to the Galápagos National Park (Table 9.1). This symmetric shield volcano reaches a maximum elevation at 760 m a.m.s.l. The satellite cinder cones are aligned in a NE-SW direction, which favors interception of SE trade winds by the windward side of the massif. The thick weathered cover in the highlands creates a smooth morphology that has been dissected by a radial drainage network with deep incisions (several tens of meters deep, clearly identifiable on high resolution satellite imagery such as Google Earth). In this area, deep incision of the landscape has been favored by a combination of factors, including island age, rock and weathered cover types, climate, and morphology. The exposure of the windward side of the massif to the SE trade winds and the large area at elevations higher than 400 m (where fog occurs) together significantly increase the volume of precipitation received on San Cristóbal's highlands, compared to those of Santa Cruz (Figure 9.6). Due to the presence of clay minerals, the weak infiltration capacity of the thick weathered cover favors concentration of the runoff, which in turn encourages erosive processes. Weathering and erosion processes have continued throughout the 2.4 Ma construction and dismantling phases of San Cristobal Island, although their intensities may have changed throughout this period.

Most hydrological studies on San Cristóbal have been focused on El Junco lake (690 m a.m.s.l.), a permanent freshwater lake and unique feature in the Galápagos Islands. Its paleo-climate records have been studied since the 1960s [*Colinvaux*, 1968; *Conroy et al.*, 2008, 2009; *Bush et al.*, 2010]. The lake occupies a volcanic crater and never empties. However, owing to a natural hydraulic threshold (i.e., the natural outlet of the lake that contributes to surface flow), and as a function of climate conditions, its water level varies by less than a meter throughout the year. In 2005, weekly monitoring of river and spring water discharge was carried out for five months (March to July) [*Adelinet*, 2005], which was a relatively dry year compared to average conditions (Figure 9.7). River water discharge was less than a few liters per second for the majority of the streams; some of them even stopped after few weeks of monitoring. The exception is the one located upstream of *Cerro Gato Captación* (River "e" on Figure 9.7), with water discharges ranging from 15–25 L/s (Figure 9.7). The streams are fed by low outflow springs (water discharges less than 0.5 L/s) and diffuse seepage along the ravines. From place to place along the river, the surface flow may disappear and contribute to deep infiltration and recharge of the underlying basal aquifer. Along the southern coastline of San

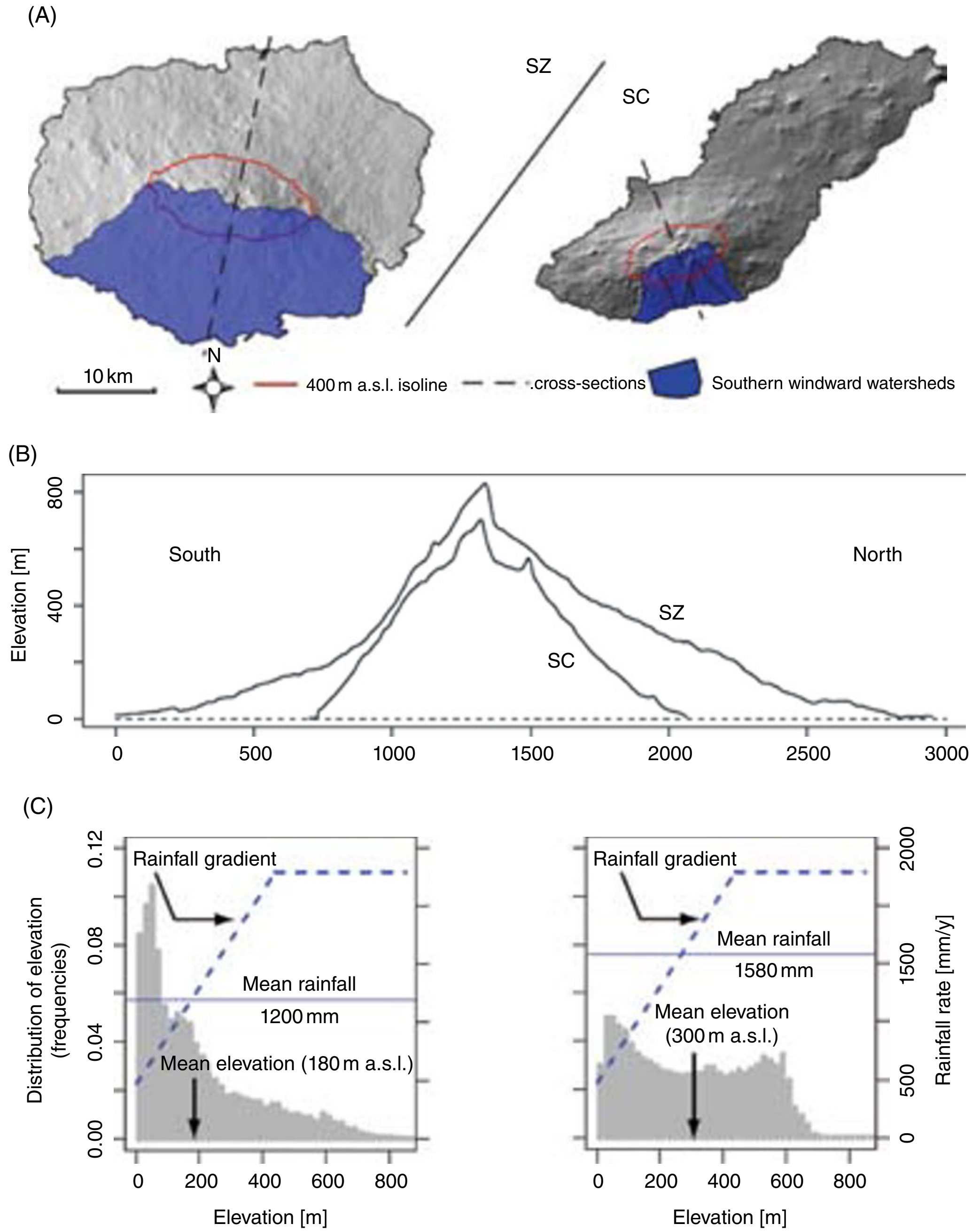

Figure 9.6 Relationship of morphology with rainfall: (A) Santa Cruz and San Cristóbal morphology maps showing the windward side of the island (blue), cross-section line (black); the elevation above 400 m subject to permanent fog during *garúa* season (red line); (B) cross-sections from (A), showing Santa Cruz and San Cristóbal morphology; (C) frequencies and spatial distribution of rainfall with elevation for Santa Cruz (left) and San Cristóbal (right), [Pryet, 2011].

Cristóbal, the mouths of rivers have three different morphologies: a lagoon at sea level, partly closed by a gravel bar; a waterfall over a cliff tens of meters above sea level; and a bedrock-floored ravine that extends all the way to the sea. Where the waterfall occurs, it is possible to observe in the cliff outcrop that an impervious layer (red baked soil) underlies the river. This impervious layer may sustain a shallow perched aquifer, favoring lateral flow in the overlying fractured lava flows, rather than a vertical flow.

9.3.4. Groundwater

Characterizing the occurrence of groundwater and quantifying it in the Galápagos Islands is the most challenging task. A basal aquifer has been identified visually through *grietas* (i.e., large, vertical, open fractures that provide access to the water level) on Santa Cruz Island (and Isabela), and is believed to exist on the other main islands, specifically on San Cristóbal. The aquifer

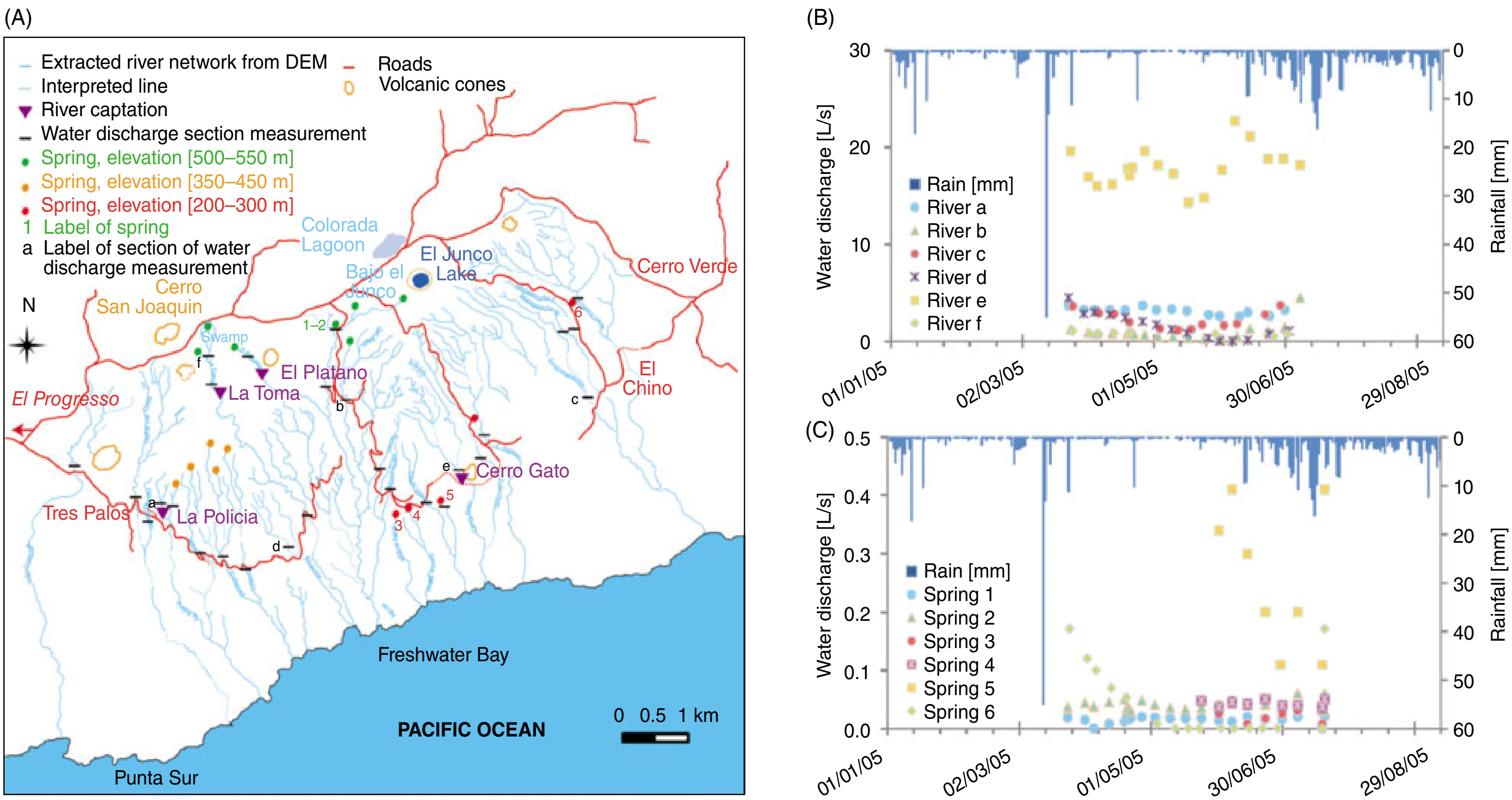

Figure 9.7 (A) Surface water drainage network on San Cristóbal extracted from DEM (SRTM) analysis and location of the main springs (reconnaissance inventory in 2005) and river water discharge measurements. Examples of water discharge temporal evolution for some springs (B) and rivers (C) between March and July 2005 [Adelinet, 2005].

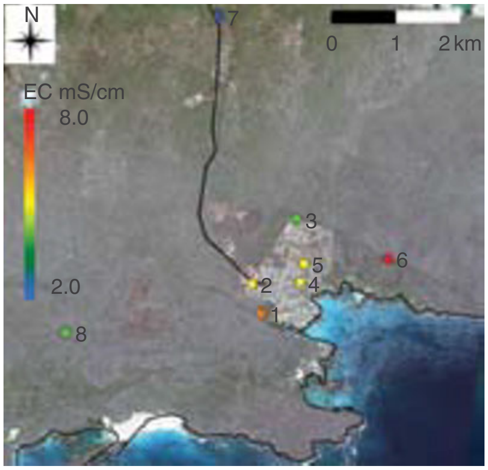

Figure 9.8 Groundwater electric conductivity of the basal aquifer measured in June 2009 in several *grietas* [Pryet et al., 2010].

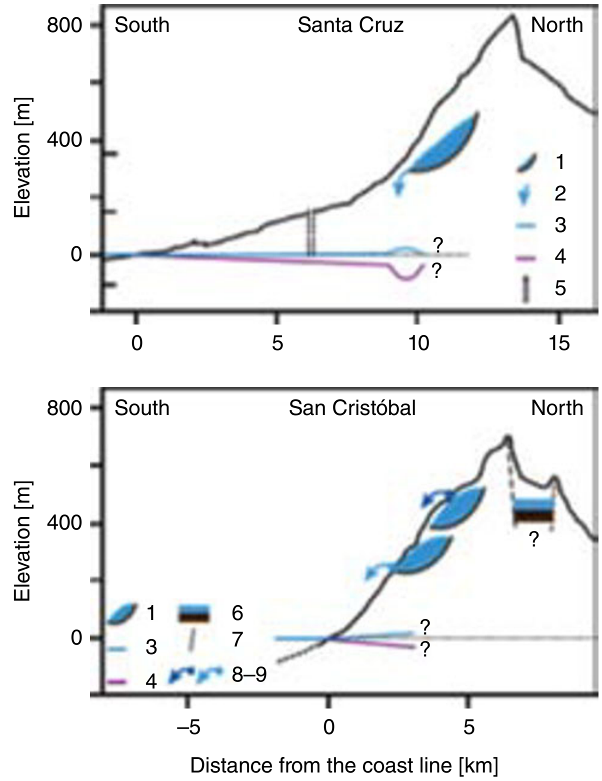

Figure 9.9 Conceptual hydrogeological model for Santa Cruz and San Cristóbal, showing their potential groundwater resources. (1) Perched aquifer; (2) preferential recharge from perched aquifer to basal aquifer; (3) water level of the basal aquifer; (4) freshwater/saltwater interface of the basal aquifer; (5) *pozo profundo*; (6) impounded dike aquifer; (8) depression spring; (9) contact spring.

is brackish—a result of seawater intrusion (Ghyben-Herzberg principle). It is also subject to anthropogenic contamination from the growing urban areas [*Liu and d'Ozouville*, 2012].

Other than on San Cristóbal (described previously), high elevation springs are reported on Santa Cruz, Floreana, and Santiago Islands. They are the result of local geological conditions (cinder or pyroclastic cones) and possess low flow rates imposed by climatic conditions. The springs identified on San Cristóbal through a nearly comprehensive survey are either perennial or ephemeral (Figure 9.7). Their origins differ from those observed on the other islands because they feed permanent or ephemeral outflow streams and their location is either in break-in-slope or depression areas, but is rarely associated with volcanic cones.

The main characteristics and hydrodynamics of the aquifers on the basaltic islands of Santa Cruz and San Cristóbal are interpreted from our field data, combined with analysis of remote sensing imagery and a comprehensive helicopter-borne geophysical survey that revealed unexpected results about the internal structure and the occurrence of aquifers within the two volcanic massifs [*d'Ozouville et al.*, 2008b; *Auken et al.*, 2009; *Pryet et al.*, 2012b].

9.3.4.1. Basal aquifer

The basal aquifer is observed on Santa Cruz through *grietas* at low elevation and at two deep boreholes located near each other at 150 m elevation: *Pozo Testigo* and *Pozo Profundo* (Figure 9.3). The groundwater electric conductivity ranges from 8.06 mS/cm at Charles Darwin Station (location 6 on Figure 9.8) to 1.95 mS/cm at *Pozo Profundo* (location 7 on Figure 9.8), located at 1.2 km and 4.8 km from the sea, respectively (measured in June 2009) [*Pryet et al.*, 2010]. In January 2003, *Pozo Profundo* groundwater had an electric conductivity of 1.53 mS/cm; the increase has been observed since its use for municipal Puerto Ayora water demand (April 2004), suggesting that the basal aquifer is overexploited and that the seawater wedge is slowly migrating inland.

According to the geophysical data [*Auken et al.*, 2009], the basal aquifer is observable around the entire island, in equilibrium with the seawater that laterally intrudes the highly pervious fractured basalt, extending up to at least 9 km inland (Figure 9.9). This wide seawater intrusion suggests that the weak hydraulic gradient, $i = 5.10^{-5}$, calculated from water level measurements between the coast and the *Pozo Testigo* borehole, is preserved inland. Resistivity mapping permits visualization of the seawater-freshwater interface, which exhibits a few depressions that may correspond to preferential recharge areas. The most prominent depression appears at the vertical projection of the hidden perched aquifer's southern boundary (see Perched aquifers, below). On the basis of the Ghyben-Hezberg relationship, a locally thicker freshwater lens floating above the seawater where recharge is occurring would deepen the freshwater-saltwater interface. The hydraulic diffusivity of the unconfined basal aquifer was determined with a 1D-analytical tidal wave propagation model to be 140 m^2/s (D = T/S, ratio of transmissivity T to storage coefficient S) [*d'Ozouville*, 2007; *Pryet*, 2011]. In basaltic media, the high discontinuity density (fractures, cooling joints, and interflow voids) induces an elevated transmissivity, but the storage coefficient is known to be low. The high discontinuity density is also confirmed by recent geophysical data collected using seismic refraction [*Loaiza et al.*, 2012].

9.3.4.2. Perched aquifers

Even though there is only one known spring on Santa Cruz Island—located at Santa Rosa at the base of a volcanic cone—the south-central side of San Cristóbal Island hosts numerous springs (Figure 9.7; see Basal aquifer, above). The high-resolution resistivity dataset, however, reveals that both islands have prominent low resistivity layers in the range of 30–130 ohm.m beneath the windward highlands. This range is of particular interest because it has been shown to be characteristic of basalt saturated by water at other basaltic islands [*Lienert*, 1991; *Descloitres et al.*, 1997; *Krivochieva and Chouteau*, 2003]. Remote sensing imagery and field data analysis have been combined with the geophysical mapping observation to identify and characterize the perched aquifers.

On Santa Cruz, the low resistivity layer (30–130 ohm.m) [*d'Ozouville et al.*, 2008b] covers an area of approximately 50 km^2 and slopes parallel to the topography in the north-south direction and gently to the east of the island in the east-west direction. Its thickness is approximately 80 m upslope and decreases to approximately 10 m downslope. The layer is "hidden," buried approximately 100 m deep, and is not exposed in outcrop. This explains the absence of springs and the presence in the underlying basal aquifer of local seawater/freshwater interface depressions (see Basal aquifer, above). The groundwater flows accordingly with the higher slope of the bedrock layer, where it encounters vertical fractures or faults that ensure indirect recharge to the basal aquifer (Figure 9.9). The perched aquifer is composed of either colluvial, inter-bedded lava flow deposits or fractured basaltic lava flows that cover pyroclastic material deposited during the shield-building phase of the volcano. These latter deposits are easily weathered to clays and could constitute an impermeable layer, especially if they were overlain by hot lava during subsequent eruptions and 'baked' to form "red layers," as has been observed on other volcanic islands around the world and in the archipelago. This thin layer (5–10 m thick), which we treat as impervious bedrock, cannot be resolved by inversion of the geophysical data.

On San Cristóbal, perennial and sporadic springs are spread over the southeastern central side of the massif at various altitudes between 200 m and 550 m elevation (Figure 9.7). Field mapping and characterization of springs has led to the identification of two types: depression springs and contact (overflow) springs. In the case of a depression spring, the incised topography cuts across the water level of a perched aquifer body. This implies that only the upper part of the aquifer is tapped by the spring. Furthermore, depending on the recharge and discharge rates of the aquifer, as well as resulting fluctuations in water level, this spring may stop flowing. Depression springs may be associated with swamp-like areas as well. In the case of a contact spring, both the water level and the impervious layer beneath a perched aquifer body intercept the incised topography. Therefore, unless the perched aquifer body dries completely, there will always be an outflow of the spring. Two types of contact springs have been identified in the field: lithological and structural. At lithological contact springs, the substratum of the perched aquifers can be red baked soil or clay layers, and the overlying aquifer flows in fractured basalt or scoria deposits. The structural contact springs are associated with faulting within the bedrock.

Generally, upslope of any spring, a low resistivity body can be identified on the 3D-resistivity bloc inversion [*Pryet et al.*, 2012b]. Nevertheless, the intrinsic geometry of these bodies appears to be complex and it remains difficult to document hydrogeological watersheds for each spring. Perennial springs have low flow rates (less than 0.5 L/s and even less than 0.1 L/s for some of them; March-June 2005; Springs 1–4 on Figure 9.7) and weak oscillations, which correspond to the smoothing effect of groundwater flow through an aquifer. This is confirmed by spring groundwater age, estimated using noble gas and isotopic tools, which indicates that the groundwater is young, less than a few years old [*Warrier et al.*, 2012]. Sporadic springs (Springs 5 and 6, Figure 9.7) can be divided into two types of hydrodynamic behavior. The first category is characterized by a wider range of flow rates with long periods of no-flow, regardless of the rainfall, indicating the possible overflow effect of an aquifer bucket. The second category of springs has sharp flow rate oscillations dictated by rainfall, indicating rapid water flow through highly fractured media—probably more influenced by non-saturated transfer. Electrical conductivities of spring groundwater remain low, ranging from 0.029–0.173 mS/cm (data collected during several campaigns between 2003 and 2009).

On the south-central windward side of San Cristóbal, the presence of flowing surface water year-round favors weathering processes even at depth through infiltration.

Thus, downstream of the spring outlets, the massif has a lower resistivity (less than 200 ohm.m, extending down to 200 m) than the one observed for unsaturated basalt (more than 800 ohm.m). This is one of the main differences between Santa Cruz and San Cristóbal Islands. The second difference concerns the presence along the northern crest of a buried, low resistivity channel (30–170 ohm.m) on San Cristóbal Island [*Pryet et al.*, 2012b]. It is bounded by two volcanic cone lineations on the surface and by sharp scarps at depth, underlain by resistivity contrasts (more than 400 ohm.m). We propose that vertical dikes supplying the volcanic cones from depth can explain the observations. The dikes could isolate an impounded, perched aquifer ideally located to benefit from recharge by rainfall on the highlands. This groundwater flow probably diverges from the summit toward the west and east, consistent with the higher bedrock slope (Figure 9.9).

9.4. DISCUSSION

This synthesis allows us to compare the hydrogeological dynamics of San Cristóbal and Santa Cruz Islands, and to identify the controlling factors that explain the differences between them. Both islands consist of the same type of basaltic volcanic rock and share the same climatic conditions. Over time, however, slight differences have lead to distinctive hydrological regimes, including:

1. Geomorphology: differences in slope, including the absence or presence of a coastal apron and orientation of the crest;
2. Near-surface lithology: thick cover of weathered pyroclasts versus thin cover of weathered basalt; and
3. Age difference: longer duration of erosion and weathering processes versus shorter ones.

First, despite the same climatic conditions and orographic gradient, San Cristóbal is estimated to receive approximately 30% more rainfall than Santa Cruz as a result of its location on the SE corner of the archipelago. Its steeper slopes are oriented perpendicular to the SE trade winds, and a greater proportion of its surface area is above 400 m elevation. Second, the thick, weathered pyroclastic cover (10 m) over the summit area of San Cristóbal favors surface flow concentration, in contrast to the Santa Cruz highlands, where infiltration processes dominate through the thin cover of weathered basalt. Third, the longer time since volcanism cessation on San Cristóbal compared to Santa Cruz has enhanced erosion processes at San Cristóbal, leading to deeper incision of the topography. This, in turn, has favored the occurrence of springs and a perennial river network. Furthermore, the greater age of San Cristóbal Island is associated with a reduction in hydraulic conductivity at depth because the basalt is more weathered [*Custodio*, 2004]. Consequently, Santa Cruz is in a younger evolutionary stage than San Cristóbal, in terms of its hydrologic development. With time, Santa Cruz is likely to become more like San Cristóbal; San Cristóbal, in turn, may evolve toward sustaining a thicker basal aquifer constrained by reduced hydraulic conductivity. According to Jefferson and co-authors (Chapter 10, this volume), volcano dissection starts between 0.5 and 2 My, depending on the climate, which is consistent with our conclusions about the hydrologic evolution of our two islands and its relationship to the age of the edifice.

When compared to other volcanic islands around the world, the hydrogeology of Santa Cruz and San Cristóbal are more consistent with the Hawaiian hydrogeological model [*Peterson*, 1972; *MacDonald et al.*, 1983]. If, however, these islands develop a thicker basal aquifer in several more million years, their behavior will more closely resemble the Canary Islands' hydrogeological model [*Custodio et al*., 1983, 1988]. As a result, we propose that an evolutionary relationship connects the two existing hydrogeological conceptual models, which are often presented in opposition to one another in the literature [*Join et al.*, 2005]. The models instead represent end-members in terms of age, between young islands (younger than 1 Ma) like Hawai'i [*Peterson*, 1972; *Mac Donald*, 1983; *Hunt*, 1996; *Gingerich et Voss*, 2005] and old ones (older than 5 Ma) like the Canaries [*Custodio et al*., 1983, 1988]. In this paradigm, Santa Cruz adheres to the Hawaiian model (valid for islands younger than 1 Ma). In contrast, San Cristóbal is in an age-advanced stage of the Hawaiian model, in the process of evolving toward the Canary Islands model (valid for islands older than 5 Ma).

We have also started studying Floreana and Isabela Islands to determine where they fall on the spectrum of Galápagos hydrogeological evolution. Floreana appears to be in a similar stage to that of Santa Cruz, with no permanent streams, several highland springs, and a well-developed drainage network on the windward side. Isabela is the youngest of the five inhabited islands and is the only one known to possess a basal aquifer with some large outflow springs near the coast (El Estero). On the windward side of this island, weathering processes are already at work, soils have developed on a lapilli substrate, and drainage networks have begun to form. On this island, that presence of groundwater has been detected through interpretation of seismic data [*O'Connor*, 2011].

9.5. RECOMMENDATIONS FOR GROUNDWATER MANAGEMENT PRACTICES IN THE GALÁPAGOS

Freshwater resources on the Galápagos Islands are limited. Our research explains why only the older island of San Cristóbal has permanent surface freshwater, and where groundwater resources are present on this and other inhabited islands. All of the water resource potential on the inhabited islands (with the exception of Baltra, a low-lying island in the wind shadow of Santa Cruz) is located on their southern windward sides. Drilling near coastal areas will systematically produce brackish water from the basal aquifer and increase risks of saltwater intrusion through over-exploitation. Further inland, water from the basal aquifer will be fresher, but drilling costs will be higher due to the increased depths of drilling required (more than 150 m). Drilling exploration for perched aquifers could be carried out on Santa Cruz Island, and, if successful, would provide an excellent source of freshwater for the community that will have to be managed properly to ensure maintenance of quality and quantity. On San Cristóbal, the exploitation of perched aquifers is not recommended, as it could pose risks to the sustainability of the stream and river network if they are over-exploited. On this island, the impounded dike aquifer might be a feasible alternative, if limited to the southwestern branch zone between El Progresso and Puerto Baquerizo Moreno. This option also reduces the length of pipes required to provide groundwater to consumers.

On Floreana and Isabela Islands, fresh water resources are expected on their windward sides. We anticipate that fresh water will be found a few kilometers inland at sea level depth as a thin basal aquifer and/or at mid-slope, a few hundred meters below the ground, as perched aquifers. In both cases, a combined exploration approach, including direct (hydro-climatologic network at watershed scale from coast to highlands and geological field surveys) and indirect (remote sensing and geophysics) methodologies, is recommended to determine the best places to drill bore wells.

For inhabited islands, water resource management practices must take into account the distinct characteristics of each island. To prevent water conflicts in the agricultural sector of the highlands, management practices must also distinguish between Galápagos National Park land and agricultural areas, as well as the specific needs of both rural and urban communities. Integrated watershed management though an inter-institutional framework is recommended to ensure protection of highland recharge areas, maintain the quality of ecosystems, ensure fair distribution of available resources within the agricultural sector (for crops or livestock management), and develop a sustainable program for water use in the urban environment. To contribute to these goals, and to work toward developing an integrated water resource management system in the Galápagos, we provide local authorities with scientific information, monitoring data, and recommendations based on results from the GIIWS project on a regular basis.

9.6. ACKNOWLEDGMENTS

The authors thank the following institutions and foundations for GIIWS project funding: Fondation de France, Fondation Entreprise Véolia Environnement, Fondation Schlumberger-SEED, Naturalia et Biologia, Université Pierre et Marie Curie, European Space Agency, Chancellerie des Universités de l'Académie de Paris, Municipality of Santa Cruz and BID-UGAFIP and ANR-blanc 2010 GIIWS Ref. 601–01. The authors are grateful for fruitful collaboration with the HGG team from Aarhus University for the SkyTEM survey and geophysical inversion. We are grateful to the Galápagos National Park Service, the Charles Darwin Foundation, the Municipalities of Santa Cruz and San Cristóbal, and the Galápagos Government Council (i.e., INGALA) for local collaborations and logistical support, and to the INAMHI for sharing climatologic data. This project is also a great opportunity to reinforce scientific collaboration with EPN-Quito and to share experiences with students from both France and Ecuador. The helpful comments and corrections from Anne Jefferson and Gordon Grant and the support from Karen Harpp are gratefully acknowledged.

REFERENCES

Adelinet, M. (2005), Etude hydrologique des bassins versants de l'île de San Cristóbal (Galápagos–Equateur), Février 2005–Août 2005, Master-thesis, Master 1 Sciences de la Planète ENS-Paris, 53p.

Adelinet, M., J. Fortin, N. d'Ozouville, and S. Violette (2008), The relationship between hydrodynamic properties and weathering of soils derived from volcanic rocks-Galápagos Islands (Ecuador), *Environ. Geol.*, *56*, 45–58, doi:10.1007/s00254-007-1138-3.

Auken, E. et al. (2009), SkyTEM contribution to hydrogeology of volcanic Islands of Galápagos Archipelago, CRAS-Geoscience, *341*, 899-907, doi:10.1016/j.crte.2009.07.006.

Bow, C.S. (1979), The geology and petrogeneses of the lavas of Floreana and Santa Cruz islands: Galápagos Archipelago, PhD-Thesis University of Oregon, 308p.

Brochet, P., and N. Gerbier (1968), L'évapotranspiration—aspect agro-météorologique, évaluation pratique de l'évapotranspiration potentielle, Monographies de la Météorologie Nationale, 65.

Bush, M.B. et al. (2010), Forty years of paleoecology in the Galápagos, *Galápagos Research*, *67*, 55–61.

CDF, SPNG, and UNM, (2004), http://www.mbs.unm.edu/herpetology/research, Data generated by Fundación Charles Darwin, Servicio Parque Nacional Galápagos and University of New Mexico.

Colinvaux, P. (1968), Reconnaissance and chemistry of the lakes and bogs of the Galápagos Islands, *Nature*, *219*, 590–194.

Collins, A. and M.B. Bush (2010), An analysis of modern pollen representation and climatic conditions on the Galápagos Islands, *The Holocene*, doi:10.1177/0959683610378874.

Conroy, J.L., J.T. Overpeck, J.E. Cole, T.M. Shanahan, and M. Steinitz-Kannan (2008), Holocene changes in eastern tropical Pacific climate inferred from a Galápagos lake sediment record, *Quat. Sci. Rev.*, *27*, 1166–1180.

Conroy, J.L. et al. (2009), Unprecedented recent warming of surface temperatures in the eastern tropical Pacific Ocean, *Nature Geosci.*, *2*, 46–50.

Custodio, E. (2004), Hydrogeology of volcanic rocks, *in*: Hydrogeology of volcanic rocks, Unesco Ed° Paris HIP program, 395–425.

Custodio, E., J. Guerra, J. Jiménez, J. Medina, and C. Soler (1983), The effects of agriculture on the volcanic aquifers of the canary islands, *Environ. Geol. 5* (4), 225–231.

Custodio, E., L. Lopez Garcia, and E. Amigo (1988), Simulation in the volcanic island of Teneriffe (Canary Island) by mathematical model, *Hydrogéologie*, n°2, 153–157.

Descloitres, M., M. Ritz, B. Robineau, and M. Courteaud (1997), Electrical structure beneath the eastern collapsed flank of Piton de la Fournaise volcano, Reunion Island: Implications for the quest for groundwater, *Water Resour. Res.*, *33*, 13–19.

d'Ozouville, N. (2007), Etude du fonctionnement hydrologique dans les îles Galápagos: Caractérisation d'un milieu volcanique insulaire et préalable à la gestion de la ressource, PhD thesis, Université Pierre et Marie Curie, France, 474 pp.

d'Ozouville, N. et al. (2008a), DEM generation using ASAR (ENVISAT) for addressing the lack of freshwater ecosystems management, Santa Cruz Island, Galápagos. Remote Sensing of Environment—Special issue on Monitoring Freshwater Ecosystems, *112–11*, 4131–4147, doi:10.1016/j.rse.2008.02.017.

d'Ozouville, N. et al. (2008b), Extensive perched aquifer and structural implications revealed by 3D resistivity mapping in Galápagos volcano, *Earth Planet. Sci. Lett.*, *269/3-4*, 517–521, doi:10.1016/j.epsl.2008.03.011.

Eden, C., and A. Timmermann (2004), The influence of the Galápagos Islands on tropical temperatures, currents and the generation of tropical instability waves, *Geophys. Res. Lett.*, *31*, L15, 308.

Geist, D., A. McBirney, and R. Duncan (1986), Geology and petrogenesis of lavas from San Cristóbal Island, Galápagos Archipelago, *Bull. Geol. Soc. Am.*, *97*(5), 555–566.

Geist, D.J., W. M. White, and A.R. McBirney (1988), Plume-asthenosphere mixing beneath the Galápagos archipelago, *Nature*, *333*, 657–660.

Gingerich, S., and C. Voss (2005), Three-dimensional variable-density flow simulation of a coastal aquifer in southern Oahu, Hawai'i, USA, *Hydrogeol. J.*, *13*(2), 436–450.

Hamann, O. (1979), On climatic conditions, vegetation types, and leaf size in the Galápagos Islands, *Biotropica*, *11*, 101–122.

Harpp, K., and D. Geist (2002), Wolf–Darwin lineament and plume–ridge interaction in northern Galápagos, *Geochem. Geophys. Geosyst. 3*(11), 1–19.

Heilweil, V.M., D.K. Solomon, S.B. Gingerich, and I.M. Verstraeten (2009), Oxygen, hydrogen, and helium isotopes for investigating groundwater systems of the Cape Verde Islands, West Africa, *Hydrogeol. J.*, *17*(5), 1157{1174, doi:10.1007/s10040-009-0434-2.

Herrera, C., and E. Custodio (2008), Conceptual hydrogeological model of volcanic Easter Island (Chile) after chemical and isotopic surveys, *Hydrogeol. J.*, *16* (7), 1329–1348, doi 10.1007/s10040-008-0316-z.

Hey, R., G. Johnson, and A. Lowrie (1977), Recent plate motions in the Galápagos area, *Bull. Geol. Soc. Am.*, *88*(10), 1385–1403.

Hildenbrand, A. et al. (2005), Isotopic approach of rainfall and groundwater circulation in the volcanic structure of Tahiti-Nui (French Polynesia), *J. Hydrol.*, *302*, 187–208.

Hunt, C.D. (1996), Geohydrology of the island of Oahu, Hawai'i: U.S. Geological Survey Professional Paper 1412-B, 54 p.

INGALA, PRONAREG, and ORSTOM (1989), Inventario cartográfico de los recursos naturales, geomorfología, vegetación, hídricos, ecológicos y biofísicos de las islas Galápagos, Ecuador, INGALA, Quito, Ecuador.

Izuka S.K., and S.B. Gingerich (2003), A thick lens of fresh groundwater in the southern Lihue Basin, Kauai, Hawai'i, USA, *Hydrogeol. J.*, *11*, 240–248.

Jefferson, A.J., K.L. Ferrier, J.T. Perron, and R. Ramalho (2014), Controls on the hydrological landscape evolution of shield volcanoes and volcanic ocean islands, Chapter 10, this volume.

Join, J.-L., J. Coudray, K. Longworth (1997), Using principal components analysis and Na/C1 ratios to trace groundwater circulation in a volcanic island: the example of Reunion, *J. Hydrol.*, *190*, 1–18.

Keller, G.V., G. Trowbridge, J.C. Murray, and C.K. Skokan (1979), Results of an experimental drill hole at the summit of Kilauea volcano, Hawai'i, *J. Volcanol. Geothermal Res.*, *5*, 345–383.

Krivochieva, S., and M. Chouteau (2003), Integrating TDEM and MT methods for characterization and delineation of the Santa Catarina aquifer (Chalco Sub-Basin, Mexico), *J. Appl. Geophys.*, *52*, 23–43.

Laruelle, J. (1967), Galápagos, Natuurwet Tijdschr, 236p.

Lienert, B. (1991), An electromagnetic study of Maui's last active volcano, *Geophysics*, *56*, 972–982.

Liu, J., and N. d'Ozouville (2012), Water contamination in Puerto Ayora: applied interdisciplinary research using *Escherichia coli* as an indicator bacteria, *Galápagos Report 2011–2012*.

Loaiza, S., J. Fortin, M. Adelinet, Y. Gueguen, and S. Violette (2012), Hydrodynamic properties of the basal aquifer of Santa Cruz Island using seismic refraction, Galápagos—Ecuador, *Geophysical Research Abstracts*, *14*, EGU2012-5571, EGU General Assembly 2012.

MacDonald, G., A. Abbott, and F.L. Peterson (1983), Volcanoes in the Sea, the Geology of Hawai'i, University of Hawai'i Press., Honolulu, 517 pp.

Marty, B., V. Meynier, E. Nicolini, E. Griesshaber, and J.P. Toutain (1993), Geochemistry of gas emanations: A case study of the Reunion Hot Spot, Indian Ocean, *Appl. Geochem.*, *8*, 141–152.

McBirney, A., and H. Williams (1969), Geology and petrology of the Galápagos Islands, Geological Society of America.

Mittelstaedt, E. and G. Ito (2005), Plume-ridge interaction, lithospheric stresses, and the origin of near-ridge volcanic lineaments. *Geochem, Geophys. Geosyst*. *6*(6), 1–20.

Morgan, W.J. (1978), Rodriguez, Darwin, Amsterdam, … , A second type of hot spot island. *J. Geophys. Res.*, *83*, 5355–5360.

O'Connor, M. (2011), Seismic features of Sierra Negra volcano, Galápagos and their effects on local freshwater resources, Senior Thesis. University of Rochester. 28 p.

Pereira, A.J.S., S. Victoria, A.M.P. Vicente, and L.J.P Neves (2007), Structural lineaments in a volcanic island evaluated through remote sensing techniques: The case of Santiago Island (Cape Verde), *Geoscience and Remote Sensing Symposium*, 2007, IGARSS 2007, IEEE International 23–28 July 2007. 1632–1635.

Peterson, F.L. (1972), Water development on tropical volcanic islands, type example: Hawai'i, Ground Water, *5*: 18–23.

Pouchan, P., F. Faissole, L. Humbert, G. Pelissier-Hermitte (1988), Aspect de l'hydrogéologie en Polynésie Française, *Hydrogéologie*, *2*, 169–182.

Prada, S.N., and M.O. da Silva (2001), Fog precipitations on the Island of Madeira (Portugal), *Environ. Geol.*, *41*, 384–389.

Pryet, A. (2011), Hydrogeology of volcanic islands: a case-study in the Galápagos Archipelago (Ecuador), PhD thesis, Université Pierre et Marie Curie, France, 310 pp.

Pryet, A., N. d'Ozouville, D. Sarango, and S. Violette (2010), El Acuífero Basal de la Isla Santa-Cruz, Galápagos, Ecuador, *Reporte científico y recomendaciones técnicas*, *Volumen I*: Aug. 2010, GIIWS, 25p.

Pryet, A. et al. (2011), 3D resistivity gridding of large AEM datasets: a step toward enhanced geological interpretation. *J. Appl. Geophys.*, *75*, 277–283, doi:10.1016/j.jappgeo.2011.07.006.

Pryet, A. et al. (2012a), Quantification of cloud water interception along a windward slope of Santa Cruz Island. *Agr. Forest Meteorol.*, *161*, 94–106. http://dx.doi.org/10.1016/j.agrformet.2012.03.018.

Pryet, A., N. d'Ozouville, S. Violette, B. Deffontaines, and E. Auken (2012b), Hydrogeological settings of a volcanic island (San Cristóbal, Galápagos) from joint interpretation of airborne electromagnetics and geomorphological observations, *Hydrol. Earth Syst. Sci.*, *16*, 4571–4579, doi:10.5194/hess-16-4571-2012,.

Sachs, J. et al. (2009), Southward movement of the Pacific intertropical convergence zone AD 1400–1850, *Nature Geosci.*, *2*, 519–525.

Scholl, M. S. Ingebritsen, C. Janik, and J. Kauahikaua (1998), Use of precipitation and groundwater isotopes to interpret regional hydrology on a tropical volcanic island: Kilauea volcano area, *Hawai'i Water Resour. Res.*, *32*, 3525–3537.

Snell, H. and S. Rea (1999), Noticias de Galápagos, *60*, 11–20.

Stieljes, L., B. Gourgand, and M. Steenhoudt (1988), Mode de circulation et de gisement de l'eau souterraine dans un volcan bouclier basaltique, exemple de l'Ile de la Réunion, milieu océanique tropical, *Hydrogéologie*, *2*, 83–94.

Trueman, M., and N. d'Ozouville (2010), Characterizing the Galápagos terrestrial climate in the face of global climate change, *Galápagos Research*, *67*, 26–37.

Violette, S., E. Ledoux, P. Goblet, and J.-P. Carbonnel (1997), Hydrologic and thermal modeling of an active volcano: the Piton de la Fournaise, Reunion, *J. Hydrol.*, *191*(1–4), 37–63.

Warrier, R.B., M.C. Castro, and C.M. Hall (2012), Recharge and source-water insights from the Galápagos Islands using noble gases and stable isotopes, *Water Resour. Res.*, *48*, W03508, doi:10.1029/2011WR010954.

White, M.W., A.R. McBirney, and R.A. Duncan, (1993), Petrology and geochemistry of the Galápagos Islands: Portrait of a pathological mantle plume, *J. Geophys. Res.*, *98*(B11), 19,533-19,563, doi:10.1029/93JB02018.

Won, J., J. Kim, G. Koh, and J. Lee (2005), Evaluation of hydrogeological characteristics in Jeju Island, Korea, *Geosci. J.*, *9*(1), 33–46.